Available online at www.sciencedirect.com
ScienceDirect
European Polymer Journal 42 (2006) 2581–2588
EUROPEAN POLYMER JOURNAL
www.elsevier.com/locate/europolj

pH-Sensitivity and pH-dependent structural change in polymeric nanoparticles of poly(vinyl sulfadimethoxine)–deoxycholic acid conjugate

K. Na [a], D.H. Lee [b], D.J. Hwang [c], H.S. Park [c], K.H. Lee [c,*], Y.H. Bae [d]

[a] *Division of Biotechnology, The Catholic University of Korea, Bucheon 420-743, Republic of Korea*
[b] *Department of Internal Medicine, Inha University, Incheon 402-751, Republic of Korea*
[c] *Department of Polymer Science and Engineering, Inha University, Incheon 402-751, Republic of Korea*
[d] *Department of Pharmaceutics and Pharmaceutical Chemistry, University of Utah, Salt Lake City, UT 84108, USA*

Received 10 February 2006; received in revised form 31 May 2006; accepted 14 June 2006
Available online 22 August 2006

Abstract

pH-Sensitive nanoparticles of poly(vinyl sulfadimethoxine) (PSDM)–deoxycholic acid (DOCA) conjugates were prepared by dialysis at pH 9.0. The average size and the critical aggregation concentration (CAC) of the nanoparticles were 340 nm and 2.5×10^{-1} g/l, respectively. The CAC decreased with decreasing pH as a result of the increase in the hydrophobic nature of the PSDM. Nanoparticle aggregation was observed at pHs ranging from 6.6 to 7.2. The photophysical characteristics of the nanoparticles were examined using a fluorescence probe technique. The microviscosity in the nanoparticle core was measured by 1,6-diphenyl-1,3,5-hexatriene (DPH). The microviscosity changed significantly with decreasing pH from 8.0 to 6.8, indicating a decrease in the rigidity of the inner cores. One interesting feature was that the microviscosity increased sharply at pHs below 6.8. This suggests that in this pH range most of the PSDM became deionized, which caused the reconstitution of new hydrophobic domains inside the nanoparticles.

Keywords: pH-Sensitive nanoparticles; Poly(vinyl sulfadimethoxine)–deoxycholic acid conjugates; Microviscosity; Interior structure

1. Introduction

Self-assembled nanoparticles from hydrophobized water-soluble polymers have attracted increasing attention on account of their potential biomedical and pharmaceutical applications [1–3]. Nanoparticles exhibit various structural and rheological features in aqueous solutions depending on the presence of water-soluble polymer, conjugated hydrophobic moiety or groups [4–6]. The formation of self-assembled nanoparticles is interpreted by a free energy-minimized structure, which shares a common feature of assembly with polymeric micelles. However, nanoparticles and polymeric micelles have a different interior structure. The interior of the polymeric

* Corresponding author. Tel.: +823 286 29507; fax: +823 286 55178.
E-mail address: polylee@inha.ac.kr (K.H. Lee).

0014-3057/$ - see front matter © 2006 Published by Elsevier Ltd.
doi:10.1016/j.eurpolymj.2006.06.008

nanoparticles consists of dispersed multiple hydrophobic island domains inside a hydrophilic sea domain due to the random association of hydrophobic moieties conjugated to the water-soluble macromolecules, while polymeric micelle have a single inner core of hydrophobic segments with a hydrophilic shell [6,7]. Nanoparticles with a moiety switching its hydrophilicity as a result of external stimuli is expected to show stimuli-responsive properties [8,9]. These properties may lead to the accumulation of nanoparticles at a disease site and a change in the drug release behavior.

It has been reported that most solid tumors and inflammatory regions in the body have a lower extracellular pH (<7.2) than the surrounding tissues and blood (pH 7.4) [10,11]. Various pH-sensitive amphiphilic materials have been synthesized to prepare pH-sensitive polymeric nanoparticles, and their pH-dependent assembling behavior has been extensively studied [12–14]. However, there are few systems that are responsive to small fluctuations in pH under physiological conditions.

This paper reports new pH-sensitive nanoparticles consisting of deoxycholic acid (DOCA), as a hydrophobic moiety, and poly(vinyl sulfadimethoxine) (PSDM), as a pH-sensitive segment. The pH-sensitivity and interior structural feature of these polymeric nanoparticles were examined using fluorescence techniques, dynamic light scattering and a zeta potentiometer.

2. Experimental

2.1. Materials and equipment

Sulfadimethoxine [4-amino-*N*-(2,6-dimethoxy-4-pyrimidynyl)benzenesulfonamide] (SDM) (Sigma), methacryloyl chloride (Sigma), deoxycholic acid (DOCA) (Sigma), *N*-hydroxysuccinimide (NHS) (Aldrich), dicyclohexyl carbodiimide (DCC) (TCI), 4-(dimethylamino)pyridine (DMAP) (TCI), pyrene (Aldrich), 1,6-diphenyl-1,3,5-hexatriene (DPH) (Aldrich) were used as received without further purification. 2-2′-Azobis(isobutyronitrile) (AIBN), dimethylsulfoxide (DMSO), methylene chloride (MC), and tetrahydrofuran (THF) were obtained from Junsei Chemical (Japan).

The ^{1}H spectra were obtained using a Bruker AC 250 spectrometer at 250 MHz. The FT-IR spectra were recorded on a Perkin–Elmer Spectrum 2000 Explorer FT-IR spectrometer.

2.2. Synthesis of PSDM–DOCA conjugates

Amine terminated semitelechelic PSDM was prepared via free-radical solution polymerization of methacryloyl SDM in DMSO in the presence of AIBN as an initiator (Scheme 1(a)). 2-Aminoethanethiol was added as a chain transfer agent. The details of the synthesis and characterization of the methacryloyl SDM and PSDM are reported elsewhere [15,16]. The activated succinimide ester of DOCA was first prepared in order to conjugate the PSDM and DOCA. DCC (2.62 g, 12.7 mmol) and DMAP (0.078 g, 0.64 mmol) were added to a stirred THF solution (110 ml) containing DOCA (5 g, 12.7 mmol) and NHS (1.46 g, 12.7 mmol). The reaction mixture was stirred at room temperature for 24 h under nitrogen (Scheme 1(b)). After filtering the dicyclohexylurea, the DOCA–NHS was obtained by column chromatography and dried at 40 °C under vacuum. The PSDM–DOCA conjugate was prepared by reacting DOCA–NHS with amine terminated PSDM (Scheme 1(c)). The synthetic procedure of the conjugate, PSDM–DOCA is as follows. A THF solution of the amine terminated PSDM (Mn: 2.1×10^3) (1.26 g, 0.6 mmol) and DOCA–NHS (0.88 g, 1.8 mmol) was stirred under reflux for 12 h in a nitrogen atmosphere. The PSDM–DOCA conjugate was isolated by column chromatography and was precipitate twice in diethyl ether.

2.3. Sample preparation

The conjugate was self-assembled into nanoparticles using a dialysis method (molecular cutoff of dialysis tubing: 1000). The conjugate (50 mg) was dissolved in 20 ml of DMSO. The solution was dialyzed against a borate buffer (NaOH, $Na_2B_4O_7$: pH 9.0) at room temperature. The dialysaltes were exchanged at 2, 6, 12, and 24 h after beginning dialysis. The solution was filtered through a 0.45 μm filter (Millipore) to remove the precipitated materials.

2.4. Particle size measurement

The average particle size distribution of the resulting nanoparticles was determined using dynamic light scattering (DLS, Malvern Instruments Series 4700, UK). The DLS experiment was performed using an argon ion laser system at a wavelength of 488 nm. The scattering angle was

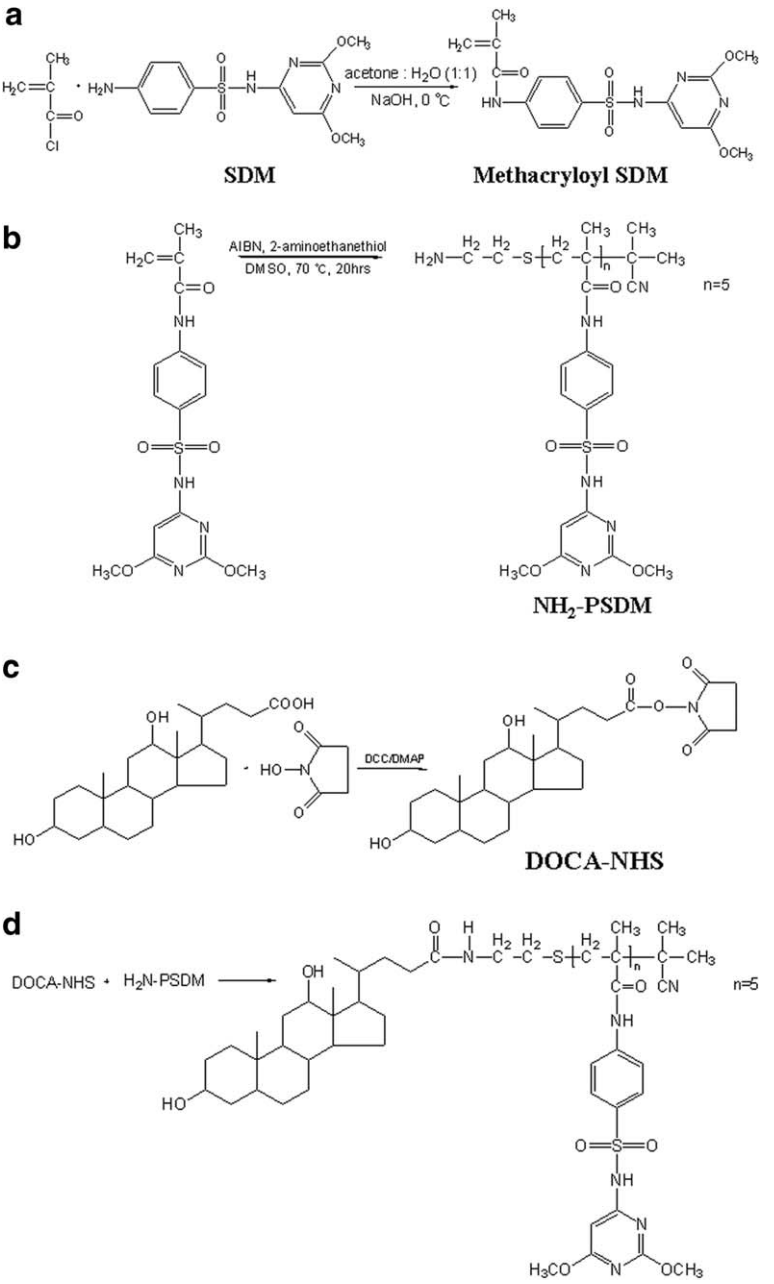

Scheme 1. Synthesis schemes of methacryloyl SDM (a), PSDM (b), DOCA–NHS (c), and PSDM–DOCA conjugate (d).

varied from 30° to 150° and the temperature was kept constant at 25 °C. The sample concentration was maintained at 1.0 g/l.

2.5. Measurement of fluorescence spectroscopy

A stock solution of pyrene (6.0×10^{-2} M) was prepared in acetone and stored at 5 °C. The steady-state fluorescence spectra were obtained by diluting the pyrene solution with distilled water to a pyrene concentration of 12.0×10^{-7} M. The solution was then distilled under vacuum at 60 °C for 1 h to remove the acetone. The acetone-free pyrene solution was then mixed with the nanoparticle suspensions, which ranged in concentration from 1×10^{-5} to 2.0 g/l. The final pyrene concentration

in the samples was 6.0×10^{-7} M, which is almost its solubility limit in water at 25 °C. The fluorescence intensity was measured using a fluorescence meter (RF-5301 PC BROC, Shimadzu, Japan).

2.6. Zeta potential measurement

The average zeta potential of the nanoparticles was determined at different pH using a zeta potentiometer (Zetasizer 3000, Malvern Instruments). The electrophoretic mobility of the nanoparticles was observed by applying an electric field of 150 V. The zeta potential was determined by varying the pH at a fixed particle concentration of 1.0 g/l.

2.7. Measurement of anisotropy value

The steady state fluorescence anisotropy values of DPH (2.1×10^{-6} M) in the nanoparticles were determined in the L-format geometry of detection. The excitation and emission wavelengths were 360 nm and 430 nm, respectively. The anisotropy value (r) was calculated using the following relationship:

$$r = \frac{(I_{VV} - I^{S}_{VV}) - G(I_{VH} - I^{S}_{VH})}{(I_{VV} - I^{S}_{VV}) + 2G(I_{VH} - I^{S}_{VH})}, \quad (1)$$

where I^S is the contribution of scattered light from a sample solution without DPH, $G(=I_{VH}/I_{HH})$ is the instrumental correction factor, and I_{VV}, I_{VH}, I_{HV}, and I_{HH} are the resulting emission intensities polarized in the vertical or the horizontal planes (second sub-index) when excited with vertically or horizontally polarized light (first sub-index), respectively.

3. Results and discussion

The PSDM–DOCA conjugate was synthesized by amine terminated semitelechelic PSDM and DOCA–NHS, which is an activated ester of DOCA. The formation of an amide linkage between the PSDM and DOCA was confirmed by the amide band in the FT-IR spectrum at 1627 cm^{-1} (Fig. 1(a)). The molecular weight was determined from the ^{1}H NMR spectrum. Fig. 1(b) shows the ^{1}H NMR spectrum of PSDM–DOCA showing the characteristic resonance peaks. The number-average molecular weight (M_n) of the PSDM–DOCA conjugate was determined by comparing the integration ratio of the portions in the DOCA part at 0.65–2.30 ppm and the methoxyl group in the PSDM at 3.8 ppm. The M_n of PSDM–DOCA was 2.48×10^3.

The critical aggregation concentration (CAC) of the PSDM–DOCA conjugate was determined using a fluorescence assay, which was based on the changes in the photophysics of pyrene that was added to the nanoparticle solution in minute amounts as a hydrophobic probe. This probe preferably partitions in a hydrophobic microenvironment. It undergoes changes in its photophysical properties as a result of the change in the micropolarity it experiences after diffusing from bulk water into the hydrophobic domains of the nanoparticle. The CAC value was estimated by monitoring the change in the ratio of the pyrene excitation spectra intensities at $\lambda = 333$ nm (I_{333} for pyrene in water) and $\lambda = 336$ nm (I_{336} for pyrene in the hydrophobic medium within the nanoparticle). Fig. 2 shows the concentration dependence of the ratio I_{336}/I_{333} at two different medium pH values. At low concentration ranges, the change in intensity ratios was negligible. The intensity ratios increase markedly with increasing concentration, which reflects the partition of pyrene into the hydrophobic domains of the nanoparticles. Hence, the CAC was determined from the crossover point at the low concentration range. The CACs of the PSDM–DOCA conjugate at pH 9.0 and pH 7.4 were 0.25 and 0.1 g/l, respectively. The CACs of the conjugate were much higher than those of other amphiphilic block copolymers. However, the values were <1.0 g/l for DOCA in water. Qualitatively it is well known that contributions from the size of the hydrophobic part and the size of the hydrophilic part of the amphiphilic molecules influence the CAC. The two contributions are counteracting, with a low CAC for a large hydrophobic part and a high CAC for a larger hydrophilic part. Therefore, the formation of nanoparticles of the PSDM–DOCA conjugate at lower concentrations indicates that the size of the hydrophobic part of the PSDM–DOCA conjugate is larger than that of DOCA. The CAC was reduced by decreasing the pH in the medium from 9.0 to 7.4. Because the CAC values are lowered with increasing hydrophobic moieties, the reduction of CAC confirms the existence of additional hydrophobic groups induced by PSDM deionization. This suggests that the secondary amine of the sulfonamide groups is well-ionized at pH 9.0, which contributes to the inter or intramolecular electrostatic repulsions. On the other hand, deionized PSDM segments encourage hydrophobic interactions at pH 7.4.

In order to further examine the pH sensitivity of the nanoparticles, the aggregation behavior of the

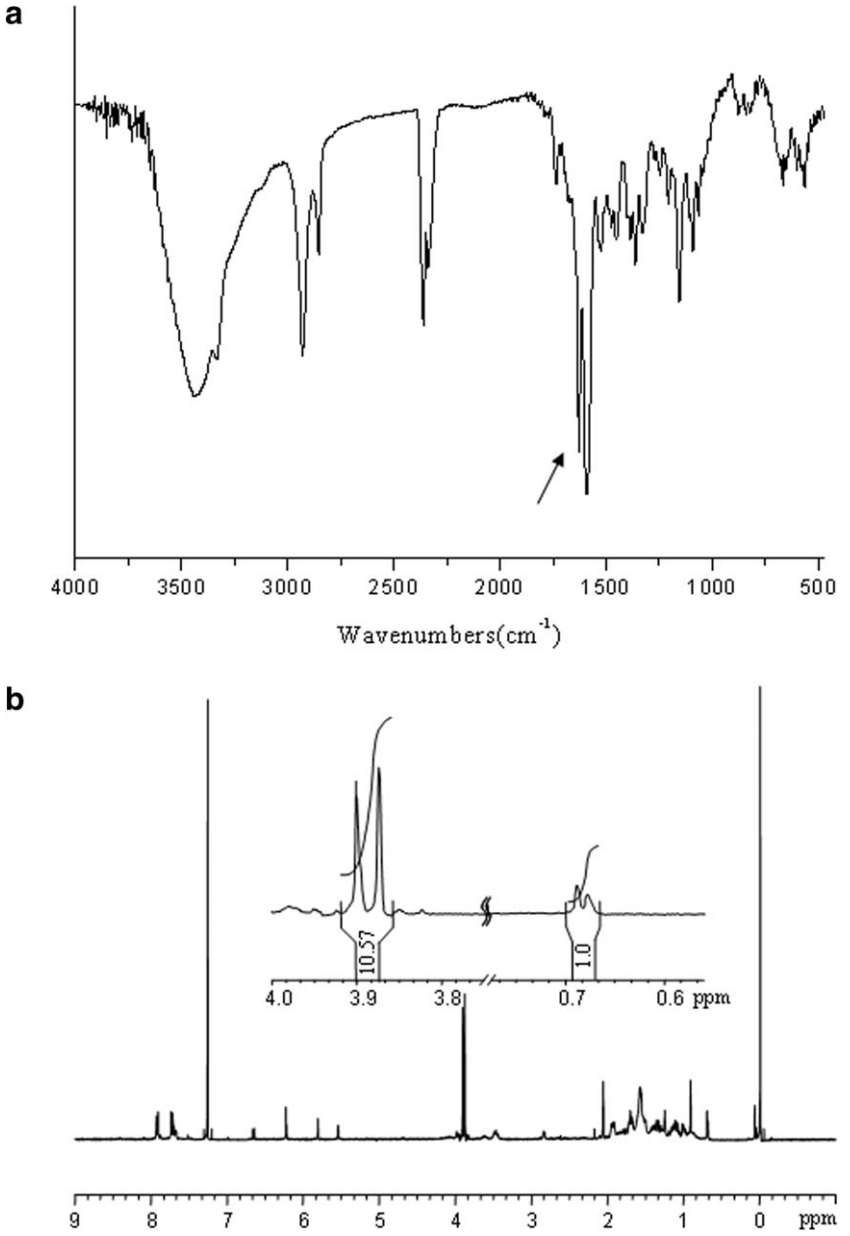

Fig. 1. FT-IR spectrum (a) and ^{1}H NMR spectrum (b) of the PSDM–DOCA conjugate.

PSDM–DOCA conjugate was investigated by measuring the particle size at various pHs. SDM is a group that influences the particle surface charge by altering the level of ionization/deionization at pHs ranging from 7.2 to 6.5. Therefore, at pH 9.0, the outer surface of the nanoparticles was presumed to be composed of ionized SDM groups. However, the deionization of SDM can lead to the pH-sensitive aggregation of the PSDM–DOCA nanoparticles because unionized SDM is known to be hydrophobic. Fig. 3 shows a dramatic change in the particle size with decreasing pH. At a high pH, the ionization of the SDM groups on the surface causes charge–charge repulsion between the nanoparticles. This can explain why the particle size was unaffected above pH 7.0. However, the particle size increased considerably from 320 nm at pH 7.2 to approximately 2000 nm at pH 6.7. This change in size with a change in the pH of 0.5 units was attributed to the aggregation of nanoparticles as a

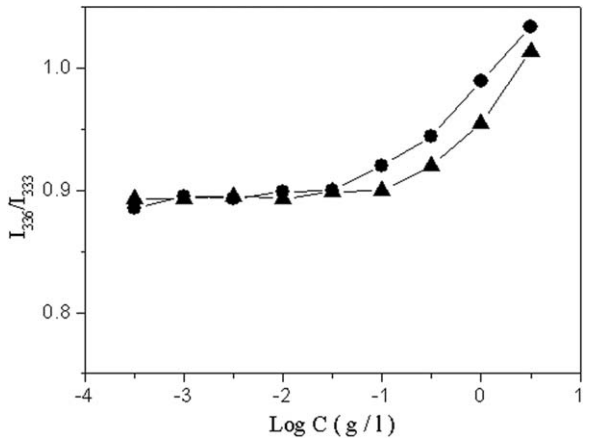

Fig. 2. Plot of I_{336}/I_{333} (from pyrene excitation spectra) versus $\log C$ for PSDM–DOCA conjugate at 25 °C. (●) pH = 7.4, (▲) pH = 9.0.

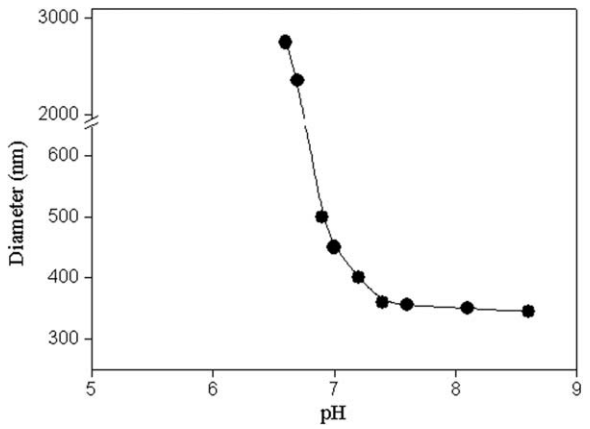

Fig. 3. Change in the particle size of the PSDM–DOCA nanoparticles as a function of pH.

result of the hydrophobic interaction due to the deionization of SDM groups on the surface. It should be noted that the transition of the particle size occurred at a relatively high pH even though the pK_a of the secondary amine of the SDM monomer is 6.1. This can be explained by the fact that when a monomer with ionizable groups is polymerized or attached to a polymer, the pK_a of the ionized groups usually shifts to a higher pH. This is because the intervening water molecules cannot provide an adequate degree of hydration for stabilizing the charged form when the hydrophobic and chargeable groups are in close proximity.

The surface charge of the nanoparticles was measured using a zeta-potentiometer in order to observe the charge density and distribution of the ionized groups on the surface as a function of pH. Fig. 4 shows the effect of pH on the zeta potential of the nanoparticles. The zeta potentials changed from −54 mV to −30 mV with decreasing pH from 9.0 to 7.2. The zeta potential values suggest that at higher pH, the fully ionized PSDM chain segment may be entirely prolonged over the water phase resulting in the formation of a broader outer shell, while at lower pH, the nanoparticles may have a relatively narrow shell as a result of the hydrophobic interactions between the deionized PSDM and DOCA parts. The results showed no change in the zeta potential between pH 7.2 and 6.6. The constant value of the zeta potential may appear contradictory because the degree of PSDM ionization should decrease with decreasing pH. However, such a trend can be explained by considering the aggregation behavior of the nanoparticles. As mentioned previously, aggregation of the PSDM–DOCA nanoparticles occurred below pH 7.2. This aggregation changed the hydrodynamic volume of the nanoparticles, which might result in an increase in the number of the ionizable SDM moieties in a single aggregate particle. This means that enlarged aggregates can provide additional ionized groups to cover the outer surface of the nanoparticles even though the degree of ionization of a single PSDM segment decreased. The increasing number of SDM moieties in a single nanoparticle due to aggregation compensated for the decreasing number of ionized groups in a single PSDM segment. Therefore, the charge density of the nanoparticles surface remained constant over a certain pH range. At lower pH, the zeta potential decreased again due to further deionization of the SDM moieties. This suggests that in

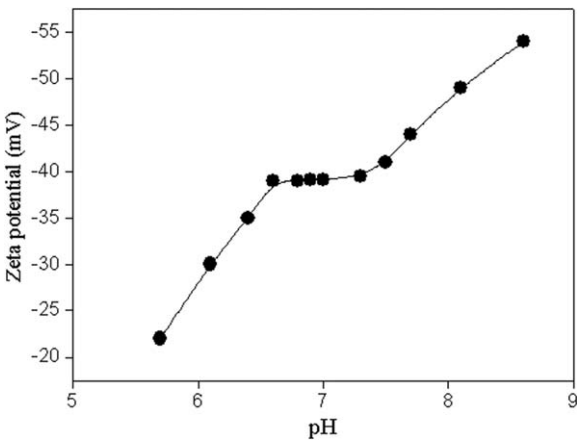

Fig. 4. Change in the zeta potential of the PSDM–DOCA nanoparticles as a function of pH.

the range of pH 6.6–5.5, the deionization process has a larger influence on the change in the surface charge density than the aggregation process.

In order to investigate the structural change in the nanoparticles, the microviscosity of hydrophobic domains were estimated by measuring the steady-state fluorescence anisotropy originating from the depolarization of the DPH fluorescence. The anisotropy increases with increasing microviscosity because the rotational diffusion of DPH is increasingly hindered. Fig. 5 shows the change in the anisotropy, r, as a function of pH. There is little difference in anisotropy at pH ranging from 9.0 to 8.0. This suggests that the stability of the hydrophobic domains was not unaffected by the change in pH in this range. However, the r value decreased significantly from 0.183 to 0.105 at pH 8.0 to pH 6.7, respectively. The reduced r value suggests a decrease in rigidity of the hydrophobic domains. This might be due to the expansion of the hydrophobic domains on account of the disruption of the hydrophobic interactions. A disruption of the hydrophilic interactions can occur as a result of the incorporation of deionized SDM moieties into the pre-existing cores. With decreasing pH, the deionized SDM should be further incorporated into the hydrophobic domains, which mainly consisted of DOCA. The incorporation of the SDM moieties might disturb the hydrophobic interaction between the DOCA units, resulting in a decrease in the microviscosity of the hydrophobic domains. Another interesting feature is that the r value sharply increased at pH 6.5. This suggests that most PSDM became deionized in this pH range and caused the reconstitution of new hydrophobic domains within the nanoparticles.

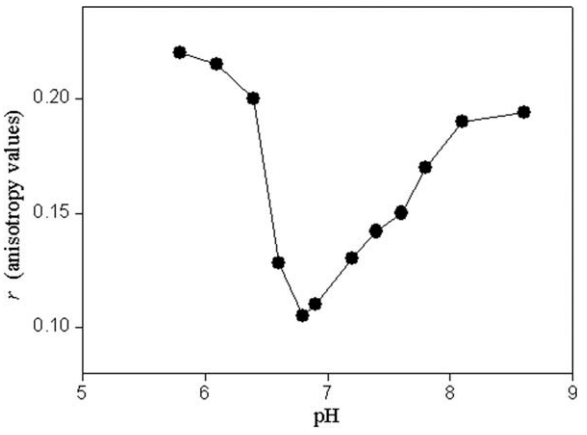

Fig. 5. Change in the anisotropy of DPH as a function of pH.

4. Conclusion

This study examined the pH-sensitivity and pH-dependent structural change of the nanoparticles of PSDM–DOCA conjugate. The results showed that at pH 9, the PSDM–DOCA conjugate formed self-assembled nanoparticles with an average size of 340 nm and a CAC of 2.5×10^{-1} g/l. Below pH 7.2, the deionization of the PSDM segments significantly lowered the charge–charge repulsion, leading to nanoparticle aggregation. Since extracellular tumor pH is slightly lower than that of normal tissue, this pH-sensitive property of the nanoparticles may provide a more effective anti-cancer drug carrier with improved passive accumulation. The increase in the total number of SDM moieties in a single particle could compensate for the decrease in the number of ionized groups in a single PSDM segment, resulting in a constant surface charge density over a certain pH range. The incorporation of deionized SDM moieties into the hydrophobic domains disturbed the hydrophobic interaction, resulting in the formation of a less condensed core structure. At a lower pH, the core composition might be significantly altered as a result of the large amount of the deionized SDM moieties incorporated in the hydrophobic domains. It was quite likely that such a change in composition caused the reconstitution of hydrophobic domains within the nanoparticles.

Acknowledgement

This research was supported by Inha University Research Grant.

References

[1] Torchilin VP. J Control Rel 2001;73:137.
[2] Janes KA, Calvo P, Alonso MJ. Adv Drug Deliv Rev 2001;47:83.
[3] Na K, Park KH, Kim SW, Bae YH. J Control Rel 2000;69:225.
[4] Nishikawa T, Akiyoshi K, Sunamoto J. J Am Chem Soc 1996;118:6110.
[5] Lee KY, Jo WH, Kwon IC, Kim YH, Jeong SY. Langmuir 1998;14:2329.
[6] Akiyoshi K, Deguchi S, Tajima H, Nishikawa T, Sunamoto J. Macromolecules 1997;30:857.
[7] Lee KY, Jo WH, Kwon IC, Kim YH, Jeong SY. Macromolecules 1998;31:378.
[8] Cammas S, Suzuki K, Sone C, Sakurai Y, Kataoka K, Okano T. J Control Rel 1997;48:157.

[9] Chung JE, Yokoyama M, Yamato M, Aoyagi T, Sakurai Y, Okano T. J Control Rel 1999;62:115.
[10] Tannock IF, Rotin D. Cancer Res 1989;49:4373.
[11] Stubbs M, McSheehy PMJ, Griffiths JR, Bashford CL. Mol Med Today 2000;6:15.
[12] Conner J, Yatvin MB, Huang L. Proc Natl Acad Sci USA 1984;81:1715.
[13] Greidziak M, Bogdanov AA, Torchilin VP, Lasch J. J Control Rel 1992;20:219.
[14] Leroux JC, Roux E, Garrec DL, Hong K, Drummond DC. J Control Rel 2001;72:71.
[15] Han SK, Na K, Bae YH. J Control Rel 2003;214:49.
[16] Na K, Lee KH, Bae YH. J Control Rel 2004;97:513.